

Mechanism and Specificity of a Symmetrical Benzimidazolephenylcarboxamide Helicase Inhibitor[†]

Craig A. Belon,[‡] Yoji D. High,[‡] Tse-I Lin,[§] Frederik Pauwels,[§] and David N. Frick^{*‡}

[‡]*Department of Biochemistry and Molecular Biology, New York Medical College, Valhalla, New York 10595, and*
[§]*HCV Research, Tibotec, Mechelen, Belgium*

Received November 16, 2009; Revised Manuscript Received January 8, 2010

ABSTRACT: This study examines the effects of 1-*N*,4-*N*-bis[4-(1*H*-benzimidazol-2-yl)phenyl]benzene-1,4-dicarboxamide ((BIP)₂B) on the NS3 helicase encoded by the hepatitis C virus (HCV). Molecular beacon-based helicase assays were used to show that (BIP)₂B inhibits the ability of HCV helicase to separate a variety of RNA and DNA duplexes with half-maximal inhibitory concentrations ranging from 0.7 to 5 μ M, depending on the nature of the substrate. In single turnover assays, (BIP)₂B only inhibited unwinding reactions when it was preincubated with the helicase–nucleic acid complex. (BIP)₂B quenched NS3 intrinsic protein fluorescence with an apparent dissociation constant of 5 μ M, and in the presence of (BIP)₂B, HCV helicase did not appear to interact with a fluorescent DNA oligonucleotide. In assays monitoring HCV helicase-catalyzed ATP hydrolysis, (BIP)₂B only inhibited helicase-catalyzed ATP hydrolysis in the presence of intermediate concentrations of RNA, suggesting RNA and (BIP)₂B compete for the same binding site. HCV helicases isolated from various HCV genotypes were similarly sensitive to (BIP)₂B, with half-maximal inhibitory concentrations ranging from 0.7 to 2.4 μ M. (BIP)₂B also inhibited ATP hydrolysis catalyzed by related helicases from Dengue virus, Japanese encephalitis virus, and humans. (BIP)₂B appeared to bind the HCV and human proteins with similar affinity ($K_i = 7$ and 8 μ M, respectively), but it bound the flavivirus proteins up to 270 times more tightly. Results are discussed in light of a molecular model of a (BIP)₂B–HCV helicase complex, which is unable to bind nucleic acid, thus preventing the enzyme from separating double-stranded nucleic acid.

All viruses need helicases to replicate their genomes, and compounds inhibiting helicases function as antiviral agents (1, 2). No helicase inhibitors have yet been approved for use in the clinic, however, and this slow development may in part be due to the fact that little is known about how most helicase inhibitors function. One of the most widely studied viral helicases is the NS3 protein encoded by the hepatitis C virus (HCV).¹ Numerous small molecules that inhibit HCV helicase have been reported, and several protein structures and mechanistic assays are available to guide compound development (3, 4). In a 1997 patent, ViroPharma Inc. reported a series of compounds inhibiting HCV helicase unwinding with half-maximal inhibitory concentration (IC₅₀) values ranging from 0.7 to 10 μ M. The ViroPharma helicase inhibitors are made of two benzimidazolephenyl derivatives that are symmetrically attached to either aliphatic or aromatic linkers (Diana, G. D., and Bailey, T. R. (1997) U.S. Patent 5,633,388). Phoon et al. later showed that both the dual benzimidazole cores and hydrophobic linker of these compounds are critical for activity, and they suggested that the compounds might act by competing with nucleic acid (5). Here, we examine

how HCV helicase and related enzymes interact with the prototype compound in the symmetrical benzimidazolephenyl series. The selected compound contains two benzimidazolephenylcarboxamide groups symmetrically linked via a benzene ((BIP)₂B, Figure 1).

HCV is a positive sense RNA virus that encodes a single ~3000 amino acid long polyprotein that is processed into 10 structural and nonstructural proteins. The HCV helicase is part of HCV nonstructural protein 3 (NS3), which like many viral proteins is multifunctional. Besides being a helicase that can unwind both RNA and DNA in reactions fueled by ATP hydrolysis, NS3 is also a protease that cleaves the viral polyprotein. The protease resides in the N-terminal NS3 functional domain, and the helicase resides in the NS3 C-terminal functional domain. Although the NS3 protein remains intact in cells, the helicase and protease can be separated *in vitro*, and these NS3 fragments retain their respective activities. The helicase fragment of the NS3 protein (called NS3h) expresses better than full-length NS3 in *Escherichia coli* and is more soluble and stable, but it unwinds RNA somewhat slower than full-length NS3 or NS3 in complex with the protease cofactor NS4A (6–8). HCV NS3h is a Y-shaped molecule with two motor domains, which are similar to those seen in all other helicases, and a third structural domain composed mainly of α -helices. One strand of nucleic acid binds in a cleft that separates the motor domains from the helical domain (9), and ATP most likely binds in the cleft separating the motor domains. A flexible linker connects the NS3 helicase and protease, which packs behind the helicase to form a cleft that binds peptide substrates (10). HCV helicase inhibitors could

[†]This work was supported by National Institutes of Health Grants AI052395 and MH085690.

^{*}To whom correspondence should be addressed. Phone: 914-594-4190. Fax: 914-594-5058. E-mail: David_Frick@nymc.edu.

¹Abbreviations: (BIP)₂B, 1-*N*,4-*N*-bis[4-(1*H*-benzimidazol-2-yl)phenyl]benzene-1,4-dicarboxamide; HCV, hepatitis C virus; MBHA, molecular beacon-based helicase assay; NS, nonstructural protein; NS3h, a NS3 protein lacking the N-terminal protease domain; YFV, yellow fever virus; JEV, Japanese encephalitis virus; DV, Dengue virus; WNV, West Nile virus.

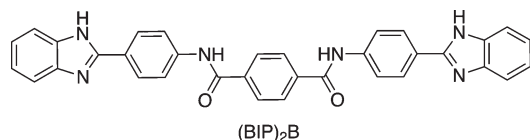


FIGURE 1: 1-N,4-N-Bis[4-(1H-benzimidazol-2-yl)phenyl]benzene-1,4-dicarboxamide, (BIP)₂B.

function by binding in place of ATP or nucleic acid, or they could bind a distant site, such as the cleft separating the protease and helicase domains. One goal of this study is to understand where (BIP)₂B might bind HCV helicase.

Antiviral compounds that target HCV enzymes should ideally inhibit all HCV varieties. The HCV species is diverse, and its members are rapidly evolving into numerous distinct genotypes whose genomes differ by as much as 35% (11). All of the various HCV genotypes respond differently to current HCV therapy (12), and many of the HCV drugs in development only target certain genotypes (13, 14).

Inhibitors designed for HCV might also target other helicases since HCV helicase shares significant homology with other motor proteins, most notably helicases encoded by similar viruses and the cellular “DEAD-box” proteins. The various HCV genotypes are part of the family *Flaviviridae*, which also contains the *flavivirus* genus that includes important human pathogens like the namesake yellow fever virus (YFV), Japanese encephalitis virus (JEV), Dengue virus (DV), and West Nile virus (WNV). Considering the sequence and structure homology seen among the *Flaviviridae* NS3 proteins (15, 16), specific inhibitors of the HCV helicase might also inhibit helicases encoded by the flaviviruses. Similarly, (BIP)₂B might interact with cellular helicases which are hijacked by other viruses to facilitate their replication. One such example is the DEAD-box protein DDX3, which is needed for human immunodeficiency virus (HIV) replication (17). Small molecules targeting DDX3 suppress HIV-1 replication (18).

Here we show that (BIP)₂B is a potent and selective inhibitor of HCV helicase and related enzymes. The compound inhibits HCV helicase-catalyzed DNA and RNA unwinding with IC₅₀ values ranging from 0.7 to 5 μM, and it most likely acts by binding in place of nucleic acid. (BIP)₂B directly binds HCV NS3h, and when bound to (BIP)₂B, HCV helicase no longer binds nucleic acids. (BIP)₂B does not directly affect NS3h-catalyzed ATP hydrolysis, but instead it blocks RNA from stimulating helicase-catalyzed ATP hydrolysis. (BIP)₂B has no effect on helicase-catalyzed ATP hydrolysis either in the absence of RNA or at saturating RNA concentrations. Since RNA binding activates ATP hydrolysis, (BIP)₂B only inhibits ATP hydrolysis at limiting concentrations of RNA. (BIP)₂B inhibits NS3h from HCV genotypes 1a, 1b, 2a, and 3a, NS3h from related human viruses, and the human DEAD-box protein DDX3. However, the compound is specific and appears to bind more tightly to some HCV genotypes than others. (BIP)₂B binds DDX3 about as well as HCV helicase, but it binds DV and JEV helicases more tightly than HCV NS3h. Results clarify the specificity and mechanism of action of (BIP)₂B. In addition, assays described here could be used to screen for more potent or active derivatives.

MATERIALS AND METHODS

Compound. 1N,4-N-Bis[4-(1H-benzimidazol-2-yl)phenyl]benzene-1,4-dicarboxamide or “(BIP)₂B” was synthesized as described

previously (Diana, G. D., and Bailey, T. R. (1997) U.S. Patent 5,633,388).

Proteins. Subcloning, expression, and purification of NS3h_1a (H77), NS3h_1b (J4), NS3h_2a (J6) (19), NS3h_1b (con1), NS3h_3a (20), NS3_1b (con1), and scNS3-4A_1b (con1) (21, 22) have been described previously. A clone of a JFH1 subgenomic replicon of HCV was obtained from Brett Lindenbach (Yale University) (23). NS3h_2a (JFH1) was subcloned from the replicon into vector pET24a (Novagen) as has been described previously for the other HCV genotypes (19, 20). A plasmid expressing NS3h from DV strain 2 was obtained from Julien Lescar (Singapore) (24), and a plasmid expressing NS3h from JEV was obtained from Bruno Canard (Marseille, France) (25). A plasmid expressing the human DDX3 protein was purchased from GenScript, Inc. (Piscataway, NJ). In the DDX3 construct, a synthetic codon-optimized open reading frame for full-length human DDX3x was placed downstream of a region encoding an N-terminal His-tagged GST fusion peptide.

All proteins were expressed in *E. coli* Rosetta (DE3) cells and purified as described previously for HCV NS3h (19). Briefly, all proteins were expressed as His-tagged proteins in 1 L cultures and purified using metal affinity, gel filtration, and ion-exchange chromatography and ammonium sulfate fractionation. Concentrations were determined by measuring A₂₈₀ using extinction coefficients determined with the program Sequence Analysis (Informagen, Greenland, NH).

Molecular Beacon-Based Helicase Assay (MBHA). MBHAs were performed using substrates shown in Figure 2A. DNA and RNA oligonucleotides were obtained from Integrated DNA technologies (Coralville, IA), annealed, and purified using polyacrylamide gel electrophoresis as described previously (22). MBHAs were initiated by rapidly mixing 10 μL of 10 mM ATP into a 90 μL of a reaction mix such that the final 100 μL reaction contained 25 mM MOPS pH 6.5, 1.25 mM MgCl₂, 5 nM substrate, 12.5 nM enzyme, 1.0 mM ATP, and 5% (v/v) DMSO. (BIP)₂B was diluted in DMSO at 20× concentration and added as 5% of the reaction mixture; control (no inhibitor) reactions included DMSO only. Enzyme was diluted in buffer containing 25 mM MOPS pH 6.5, 1 mM DTT, 0.1 mg/mL BSA, and 0.2% Tween 20 to 20× final concentration and comprised 5% (v/v) of the reaction mixture. Reactions were performed at 23 °C in low volume white 96-well microplates and monitored with a Varian Cary Eclipse fluorescence spectrophotometer. Cy5- and Tye⁶⁶⁵-labeled substrates were measured at excitation wavelength 643 nm (5 nm slit) and emission wavelength 667 nm (10 nm slit); Cy3-labeled substrates were measured at excitation wavelength 552 nm (5 nm slit) and emission wavelength 570 nm (10 nm slit). Under these conditions, the substrate is typically fully unwound in 30 min. Each reaction was performed in triplicate. Error bars in all figures mark one standard deviation, and points are the means of the three reactions.

To judge compound potency, inhibition % was first calculated using eq 1

$$\text{inhibition \%} = \frac{\frac{F_{i30}}{F_{i0}} - \frac{F_{c30}}{F_{c0}}}{1 - \frac{F_{c30}}{F_{c0}}} \times 100 \quad (1)$$

where F_{c0} is fluorescence of the control reaction (no inhibitor, DMSO only) at time zero, F_{c30} is the fluorescence of the control

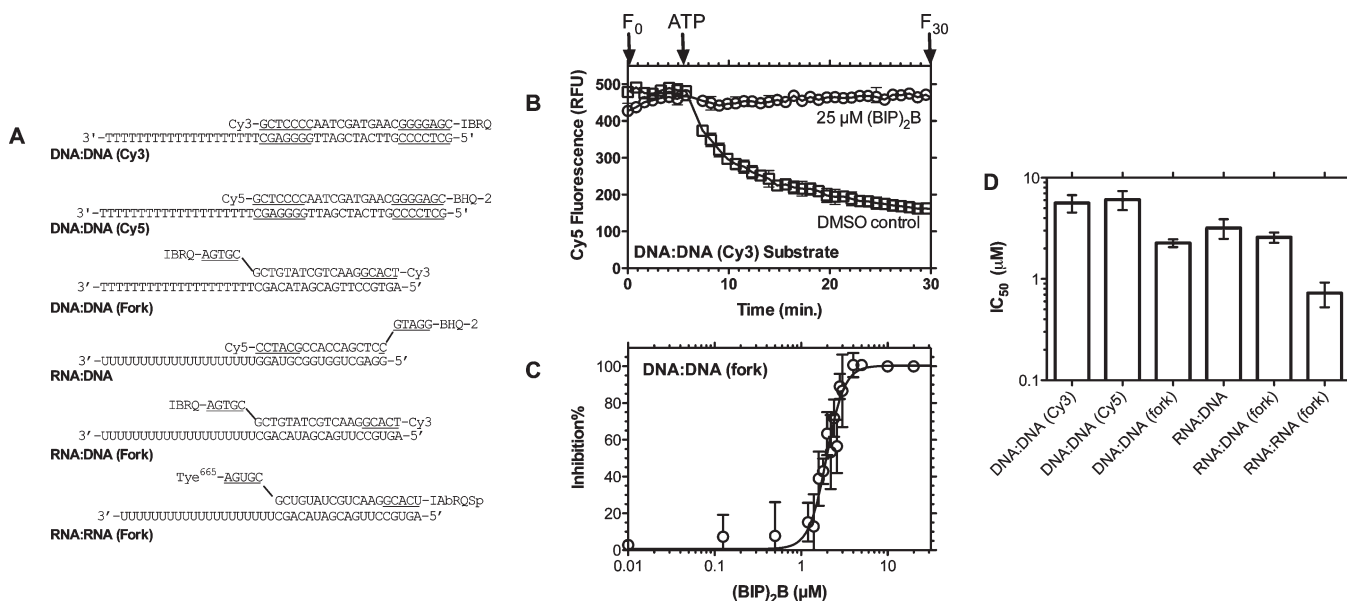


FIGURE 2: Effect of (BIP)₂B on HCV helicase-catalyzed DNA and RNA unwinding. (A) MBHA substrates used in this study. Regions forming hairpin structures after strand separation are underlined. (B) A representative MBHA using the DNA-DNA substrate in the presence (circles) or absence (squares) of 25 μ M (BIP)₂B. The arrow shows when ATP was added. Error bars represent standard deviations of three independent reactions. (C) Inhibition of HCV NS3h-catalyzed substrate unwinding by (BIP)₂B. Fluorescence measurements at time zero, F_0 , and 30 min, F_{30} , are used to compute inhibition percent with eq 1, which is plotted for the DNA-DNA (fork) substrate versus (BIP)₂B concentration. Error bars represent the standard deviation of three independent reactions. Points are fit to eq 2. (D) Concentration of (BIP)₂B required to inhibit 50% of NS3h-catalyzed strand separation in MBHAs using indicated substrates. IC_{50} values plotted are averages of three values that were determined from three independent titrations with (BIP)₂B. Errors are standard deviations.

reaction at 30 min, F_{i0} is the fluorescence of the reaction with (BIP)₂B at time zero, and F_{i30} is the fluorescence of the reaction with (BIP)₂B at 30 min. IC_{50} values were then calculated using the program Prism 5.0 (GraphPad Software) by fitting plots of inhibition % versus $\log[(BIP)_2B]$ using eq 2:

$$\text{inhibition \%} = \frac{100}{1 + 10^{n(\log IC_{50} - \log [I])}} \quad (2)$$

where n is the hillslope coefficient and $[I]$ is (BIP)₂B concentration.

Single turnover reactions were performed using a rapid mixing stopped-flow device (Applied Photophysics) with the same reagent concentrations as described above for a standard MBHA, with the addition of a final concentration of 1 μ M of the short oligo dT₂₀ in the ATP mixture to prevent the enzyme from rebinding substrate (22). Single turnover data was fit to a two-phase exponential equation:

$$\text{product} = A_{\text{slow}}(1 - e^{-k_{\text{slow}}t}) + A_{\text{fast}}(1 - e^{-k_{\text{fast}}t}) \quad (3)$$

In eq 3, “product” is the concentration of products determined as described before (22), A_{slow} and A_{fast} are the amplitudes of the slow and fast phases, respectively, and k_{slow} and k_{fast} are the rate constants for the slow and fast phase, respectively.

Ligand Binding (Intrinsic Protein Fluorescence). Aliquots of (BIP)₂B were added to three different concentrations of NS3h (50, 100, 200 nM). Both (BIP)₂B and NS3h were dissolved in the same buffer (25 mM MOPS, pH 6.5, 1.25 mM MgCl₂, and 1.0% Tween 20), the initial volume was 2 mL, and the titrations were performed in a temperature-controlled 1 cm cuvette at 23 °C. Intrinsic protein fluorescence was monitored by exciting the sample at 280 nm and reading emission at 340 nm. Excitation and emission slit widths were set to 5 and 10 nm, respectively.

All raw fluorescence data were corrected for sample dilution and inner filter effects using eq 4:

$$F = F_{\text{obs}} \left(\frac{V_0 + V_i}{V_0} \right) \times 10^{(A_{\text{ex}} + A_{\text{em}})/2} \quad (4)$$

where F is corrected fluorescence, F_{obs} is observed fluorescence, V_0 is initial sample volume, V_i is total volume of titrant added, A_{ex} is the absorbance of the solution at (BIP)₂B at the excitation wavelength (280 nm), and A_{em} is the absorbance of the solution at the emission wavelength (340 nm). (BIP)₂B absorbs light both at 280 nm ($\epsilon_{280} = 19.6 \text{ mM}^{-1} \text{ cm}^{-1}$) and at 340 nm ($\epsilon_{340} = 34.7 \text{ mM}^{-1} \text{ cm}^{-1}$). The extinction coefficient for NS3h at 280 nm is $51.8 \text{ mM}^{-1} \text{ cm}^{-1}$, but NS3h does not absorb light at 340 nm.

An equilibrium constant describing the dissociation of (BIP)₂B and NS3h was calculated by globally fitting three data sets to eq 5 using nonlinear least-squares regression analysis.

$$F = F_f \left(\frac{K_d + [I]_T + [E]_T - \sqrt{(K_d + [I]_T + [E]_T)^2 - 4[I]_T[E]_T}}{2} \right) + F_c \left(\frac{K_d + [I]_T + [E]_T - \sqrt{(K_d + [I]_T + [E]_T)^2 - 4[I]_T[E]_T}}{2} \right) + \text{BKG} \quad (5)$$

In eq 5, F is the corrected fluorescence from eq 4, K_d is the dissociation constant of the (BIP)₂B-NS3h complex, $[I]_T$ is the total (BIP)₂B concentration, $[E]_T$ is total NS3h concentration, F_f is a coefficient describing the fluorescence of free NS3h, F_c is a coefficient describing the fluorescence of a (BIP)₂B-NS3h complex, and BKG is background fluorescence.

Ligand Binding (DNA Fluorescence). Fluorescence increase of the DNA oligonucleotide F18 (5'-GCC TCG CTG

CCG TCG CCA-FAM-3') upon binding to NS3h was used to estimate the effect of (BIP)₂B on the binding of DNA to NS3h (6). To this end, DNA oligonucleotide fluorescence was monitored at an excitation wavelength of 492 nm and an emission wavelength of 518 nm, with 5 and 10 nm slit widths, respectively. A 2 mL solution of 2 nM F18 in 25 mM MOPS, pH 6.5, 1.25 mM MgCl₂, 1% Tween 20, and 1% (v/v) DMSO at 23 °C was titrated with NS3h dissolved in the same buffer. (BIP)₂B was added such that the final concentration of (BIP)₂B was 0, 0.5, and 2.5 μM. Raw data were first corrected for dilution and inner filter effects using eq 4, and the corrected fluorescence (F) at each enzyme concentration was globally fit to a model that assumed (BIP)₂B binds NS3h to form a (BIP)₂B–NS3h (EI) complex, which itself is not able to bind DNA (eq 6).

$$F = F_i + F_{\max} \left(\frac{(K_d + [D]_T + [E]) - \sqrt{(K_d + [D]_T + [E])^2 - 4[D]_T[E]}}{2[D]_T} \right) \\ \text{where } [E] = [E]_T \\ - \left(\frac{(K_i + [I]_T + [E]_T) - \sqrt{(K_i + [I]_T + [E]_T)^2 - 4[I]_T[E]_T}}{2} \right) \quad (6)$$

In eq 6, [D]_T is the concentration of F18 DNA, F_i is the observed fluorescence in the absence of added NS3h, F_{max} is the maximum change in fluorescence in each titration, [I]_T is the total (BIP)₂B concentration, and [E]_T is the NS3h concentration.

ATP Hydrolysis Assays. To examine the effect of (BIP)₂B on helicase-catalyzed ATP hydrolysis, the liberation of inorganic phosphate from ATP was monitored using a malachite green-based colorimetric assay (21, 22, 26). Unless otherwise noted, reactions were performed at 23 °C in 25 mM MOPS, pH 6.5, 5 mM MgCl₂, 1.0 mM ATP, and 2 nM NS3h, initiated by adding enzyme as 10% of the reaction mixture, after enzyme was diluted into a dilution buffer (25 mM MOPS, pH 6.5, 1 mM DTT, 0.1 mg/mL BSA, 0.2% Tween 20). Total reaction volume was 50 μL, and various amounts of poly(U) (2500 nt average length; Sigma) RNA were added. Concentrations of RNA are reported in terms of nucleotide concentration (i.e., uridine monophosphate). Absorbance at 630 nm was converted to concentration of liberated phosphate using a standard curve. Reaction velocity in nanomolar per second was determined by dividing concentration of liberated phosphate by reaction time. Specific activity, *v*/*E* (s^{−1}), was determined by dividing reaction velocity by enzyme concentration (nM).

To examine how (BIP)₂B affects the ability of RNA to activate helicase-catalyzed ATP hydrolysis, reactions were performed at various (BIP)₂B and RNA concentrations. Since (BIP)₂B affected mainly the observed affinity for the activating RNA, data were fit to a model where RNA and (BIP)₂B compete for the same site on the enzyme:

$$v/E = \frac{k_{\text{stim}}[\text{RNA}]}{K_{\text{RNA}} \left(1 + \frac{[I]}{K_i} \right) + [\text{RNA}]} + k_{\text{basal}} \quad (7)$$

where *v*/*E* is specific activity, [RNA] is poly(U) RNA concentration, *k*_{stim} is a rate constant describing maximal rate of stimulated ATP hydrolysis, *K*_{RNA} is a dissociation constant describing binding of RNA to the enzyme, *k*_{basal} is a rate constant describing the rate of enzyme-catalyzed ATP hydrolysis in the absence of

RNA, [I] is (BIP)₂B concentration, and *K*_i is a dissociation constant describing binding of (BIP)₂B to the enzyme.

To examine how (BIP)₂B competes with substrate ATP, reactions were performed at various (BIP)₂B and ATP concentrations in the presence of 15 μM poly(U). Data were fit to the Michaelis–Menten equation to estimate an apparent *K*_m and *V*_{max} at various (BIP)₂B concentrations:

$$v = \frac{V_{\text{max(app)}}[\text{ATP}]}{K_{\text{m(app)}} + [\text{ATP}]} \quad (8)$$

where *v*/*E* is specific activity, [ATP] is ATP concentration, *k*_{stim} is a rate constant describing maximal rate of stimulated ATP hydrolysis, *K*_m is a dissociation constant describing binding of ATP to the enzyme, [I] is (BIP)₂B concentration, and *K*_i is a dissociation constant describing binding of (BIP)₂B to the enzyme or the enzyme–ATP complex.

ATPase assays were performed under slightly modified conditions to compare the effect of (BIP)₂B on HCV NS3h to related helicases, which were notably less active than HCV helicase at pH 6.5 and 23 °C. To compare the effect of (BIP)₂B on HCV NS3h_1b (con1), DV NS3h, JEV NS3h, and human DDX3, reactions were instead performed in 25 mM HEPES, pH 7.5, 5 mM MgCl₂, and 1.0 mM ATP. Enzyme was again added as 10% of the reaction mixture, but after enzyme was diluted into a different dilution buffer (25 mM Tris, pH 8.0, 1 mM DTT, 0.1 mg/mL BSA, 0.2% Tween 20). Reactions were incubated for 15 min at 37 °C, terminated, and analyzed as described above. To calculate the affinity of each enzyme for RNA, specific activities observed at various RNA concentrations were fit to a modified one-site binding equation:

$$v/E = \frac{k_{\text{stim}}[\text{RNA}]}{K_{\text{RNA}} + [\text{RNA}]} + k_{\text{basal}} \quad (9)$$

where *v*/*E* is specific activity, [RNA] is RNA concentration, *k*_{stim} is a rate constant describing maximal rate of stimulated ATP hydrolysis, *K*_{RNA} is a dissociation constant describing binding of RNA to the enzyme, and *k*_{basal} is a rate constant describing the rate of enzyme-catalyzed ATP hydrolysis in the absence of RNA.

Since (BIP)₂B and RNA seem to compete for the same binding site, data were fit to a competitive inhibition model:

$$v/E = \frac{k_{\text{stim}}[\text{RNA}]}{K_{\text{RNA}} \left(1 + \frac{[I]}{K_i} \right) + [\text{RNA}]} + k_{\text{basal}} \quad (10)$$

where *v*/*E* is specific activity in the absence of the inhibitor, *k*_{basal} is a rate constant describing the rate of enzyme-catalyzed ATP hydrolysis in the absence of RNA (determined above), *k*_{stim} is a rate constant describing the maximal rate of ATP hydrolysis, *K*_{RNA} is a dissociation constant describing binding of RNA to the enzyme (determined above), [I] is (BIP)₂B concentration, and *K*_i is a dissociation constant describing the binding of (BIP)₂B to the enzyme.

Molecular Modeling. Rigid ligand docking was performed using UCSF DOCK 6.3 under academic license (<http://dock.compbio.ucsf.edu>) with PDB file 1A1V (9) stripped of its DNA ligand and water and further prepared using Dock Prep in UCSF Chimera (<http://www.cgl.ucsf.edu/chimera>). Molecular surfaces were generated using the program dms (<http://www.cgl.ucsf.edu/Overview/software.html#dms>). The potential docking site was defined as a volume within 3 Å of the oligonucleotide bound in

PDB file 1A1V. The PDB file for the (BIP)₂B ligand was generated using the free online version of CORINA (<http://www.molecular-networks.com>).

RESULTS

Effect of (BIP)₂B on HCV Helicase-Catalyzed DNA and RNA Unwinding. HCV helicase's biological substrate is not known, but the most likely candidate is the HCV genome itself, which is made only of RNA. Unlike related proteins, HCV helicase unwinds both RNA and DNA duplexes, and this uniquely promiscuous substrate specificity allows one to monitor its activity with a wide variety of substrates. If a compound inhibits the ability of a helicase to unwind a variety of substrates, it is unlikely that compound inhibits the enzyme strictly by binding the substrate rather than the enzyme itself. Therefore, to probe how (BIP)₂B inhibits HCV helicase, we used a variety of DNA–DNA, RNA–DNA, and RNA–RNA substrates (Figure 2A) and monitored HCV helicase-catalyzed DNA and RNA unwinding using the recently developed molecular beacon-based helicase assay (MBHA) (27). An MBHA monitors the ability of a helicase to displace a molecular beacon annealed to a longer oligonucleotide. MBHA substrates used here share a single-stranded tail required by HCV NS3h, but they differ in the length of the duplex region, nucleotide sequence, backbone composition (RNA or DNA), and the nature of the fluorophores and quenchers (Figure 2A). In MBHAs the fluorescence signal remains unchanged until ATP is added, activating the enzyme. When the enzyme displaces the beacon, the nucleic acid forms a hairpin bringing the quencher moiety closer to the fluorophore, causing a measurable decrease in fluorescence. In control reactions, complete separation typically occurs after approximately 30 min, but in the presence of 25 μ M (BIP)₂B, no unwinding is observed at this time (Figure 2B).

MBHAs with each substrate were performed in triplicate with various concentrations of (BIP)₂B (ranging from 0.01 to 20 μ M), and the amount of fluorescence remaining after 30 min was used to calculate percent inhibition (eq 1). Reactions were performed with 10–20 (BIP)₂B concentrations, in triplicate. Plots of percent inhibition at various (BIP)₂B concentrations were then used to determine IC₅₀ values for each substrate (Figure 2C). (BIP)₂B inhibited separation of all substrates tested, suggesting that inhibition is not due to a (BIP)₂B interaction with the nucleic acid backbone, a particular base pair sequence, or a particular fluorophore.

It is widely recognized that HCV helicase unwinds DNA better than RNA, in part, because RNA binds weaker to the NS3h protein (6). Interestingly, helicase-catalyzed unwinding of better HCV helicase substrates, i.e., those composed of DNA, was less sensitive to (BIP)₂B inhibition than unwinding of poor HCV helicase substrates, i.e., those composed of RNA. For example, inhibition of unwinding of the DNA–DNA substrate was least potent, with an IC₅₀ of 5.4 ± 0.2 μ M. When the strand along which the helicase likely tracks (i.e., the long strand) was changed to RNA, potency increased slightly to an IC₅₀ of 3.6 ± 0.1 μ M (RNA–DNA) or 2.2 ± 0.1 μ M (RNA–DNA(fork)). When both strands of the substrate nucleic acid were RNA, (BIP)₂B inhibited HCV NS3h-catalyzed RNA unwinding with the greatest potency, with an IC₅₀ of 0.7 ± 0.1 μ M (Figure 2D).

Effect of (BIP)₂B on Unwinding Reactions Performed under Single Turnover Conditions. Because of the complex nature of helicase unwinding assays, it is difficult to assess exactly how (BIP)₂B inhibits unwinding reactions. In a standard MBHA,

the enzyme is supplied in a slight excess of the substrate, and it is free to rebind partially unwound substrates after it dissociates. Since MBHA reactions are performed with excess enzyme, it is also not possible to determine if the inhibitor competes with the substrate using standard steady-state kinetics. To simplify analysis, we therefore performed MBHAs under single turnover (i.e., pre-steady-state) conditions. In single turnover MBHAs, reactions are initiated by adding ATP and an enzyme trap. The enzyme trap, the oligonucleotide dT₂₀, binds free enzyme, and enzyme that falls from the substrate before or after the beacon is displaced. Since the NS3h–DNA complex is preformed, the enzyme has only one opportunity to unwind the substrate to completion (a single turnover). After falling from the substrate, the large excess of dT₂₀ “traps” the enzyme, preventing rebinding of any unwound substrate remaining in the reaction mixture. Any observed unwinding is thus the result of a single turnover of the enzyme. All reactions were performed in a stopped-flow apparatus so that single rapid reaction cycles could be accurately monitored.

In single turnover MBHAs, a compound can be added either to the enzyme–DNA mixture, which is present in one syringe of the stopped-flow apparatus, or to the ATP–trap mixture, which is in the second syringe. If a compound binds in place of nucleic acid, one would expect to see inhibition only when the compound is added to the enzyme–DNA mixture. If a compound binds to the ATP-binding site or another site, it should inhibit unwinding when added to either syringe of the stopped-flow apparatus. When (BIP)₂B was added to the syringe containing NS3h and the 25 base pair DNA–DNA substrate, roughly the same amount of inhibition was seen as when (BIP)₂B was included in standard MBHAs (Figure 3A), suggesting that (BIP)₂B could be interacting with NS3h or the NS3h–DNA complex. In stark contrast, when (BIP)₂B was added to the ATP–trap solution, no inhibition was observed (Figure 3B), suggesting that (BIP)₂B likely does not bind the preformed helicase–DNA complex and most likely does not bind the ATP-binding site either.

Further insights into the impact of (BIP)₂B on helicase-catalyzed unwinding reactions can be gained if the time courses of single turnover reactions are fit to rate equations. Because there is a short lag to the reaction, time courses fit best to a two-phase rate equation (eq 5). Such an analysis reveals that (BIP)₂B mainly affects the amplitude of the fast phase of the reaction (Table 1). The amplitude of the reaction is proportional to both the amount of enzyme bound to the substrate when the reaction is started and the reaction processivity, which is defined as the likelihood that the helicase will displace the beacon before it dissociates from the substrate. This experiment alone does not differentiate whether (BIP)₂B affects binding or processivity. However, these experiments clearly indicate that (BIP)₂B does not bind in place of ATP. If it did, one would expect to see some dose dependency in experiments where unwinding was initiated with ATP and inhibitor.

Evidence of a Direct (BIP)₂B–NS3h Interaction. We next sought to examine if (BIP)₂B could directly bind HCV helicase in the absence of the DNA and ATP substrates. If (BIP)₂B binds HCV helicase at the known DNA binding site (9), one might expect the compound to quench intrinsic protein fluorescence. Quenching should occur because (BIP)₂B absorbs light at 340 nm, the peak emission wavelength for tryptophan fluorescence. A solvent-exposed tryptophan (W501) flanks the known NS3 DNA binding site, and DNA binding to NS3h causes clear changes in intrinsic NS3h fluorescence (28, 29). If (BIP)₂B

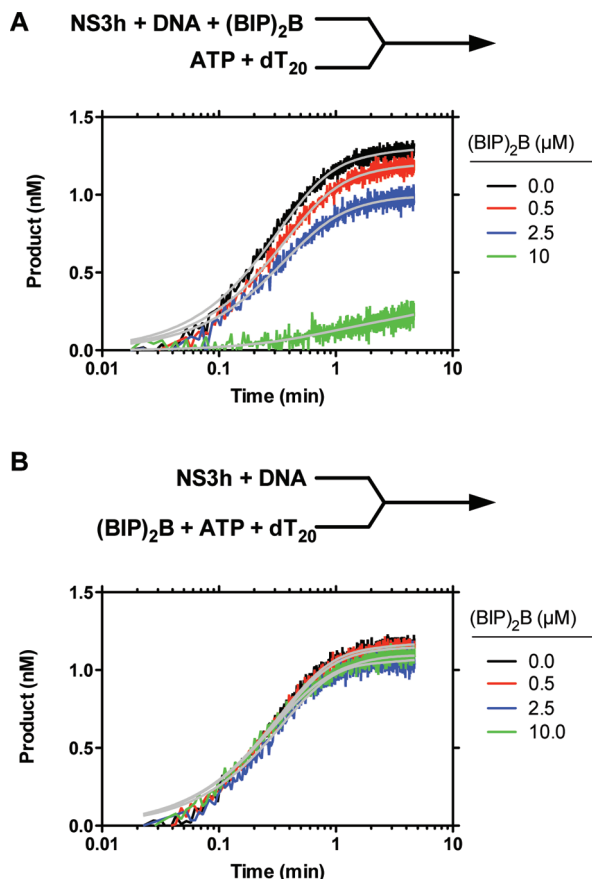


FIGURE 3: Effect of $(\text{BIP})_2\text{B}$ on HCV-catalyzed DNA unwinding in the presence of a protein trap (single turnover conditions). Pre-steady-state time courses for NS3h_1b (con1) catalyzed DNA–DNA MBHAs performed in the presence of 0, 0.5, 2.5, or 10 μM $(\text{BIP})_2\text{B}$ and 1 μM dT_{20} (enzyme trap). All time courses shown represent the average of four independent experiments. Error bars are omitted for clarity. (A) A syringe containing enzyme, DNA, and $(\text{BIP})_2\text{B}$ is mixed with a syringe containing ATP and dT_{20} to initiate unwinding such that final concentrations of all reagents are the same as in a standard helicase reaction. (B) A syringe containing enzyme and DNA (preformed E–DNA complex) is mixed with a syringe containing $(\text{BIP})_2\text{B}$, ATP, and dT_{20} to initiate unwinding. Data are fit to eq 3 with the constants in Table 1.

Table 1: Rate Constants Determined from Single Turnover MBHAs^a

$(\text{BIP})_2\text{B}$ (μM)	A_{slow} (nM)	k_{slow} (min^{-1})	A_{fast} (nM)	k_{fast} (min^{-1})
0	0.17 ± 0.07	0.70 ± 0.30	1.1 ± 0.11	3.2 ± 0.21
0.5	0.19 ± 0.8	0.70 ± 0.30	1.0 ± 0.12	2.9 ± 0.23
2.5	0.20 ± 0.13	0.78 ± 0.38	0.78 ± 0.13	3.0 ± 0.41
10	0.17 ± 0.07	0.26 ± 0.25	0.10 ± 0.09	1.7 ± 1.6

^aFour separate reactions were performed at various different $(\text{BIP})_2\text{B}$ concentrations using the DNA–DNA MBHA substrate, as described in Materials and Methods and shown in Figure 3. Each parameter is the average of four parameters determined from four fitted reactions. Errors are standard deviations.

binds the same site, it should cause a similar fluorescence decrease. In order to determine if $(\text{BIP})_2\text{B}$ directly binds NS3h, we therefore measured the fluorescence of NS3h at various fixed concentrations of NS3h in the presence of increasing amounts of $(\text{BIP})_2\text{B}$ (Figure 4A). After correcting for dilution of NS3h and inner filter effects (eq 4), data were fit to a model where the fluorescence of free enzyme is proportional to a constant, F_f , and fluorescence of the $(\text{BIP})_2\text{B}$ –NS3h complex is proportional to

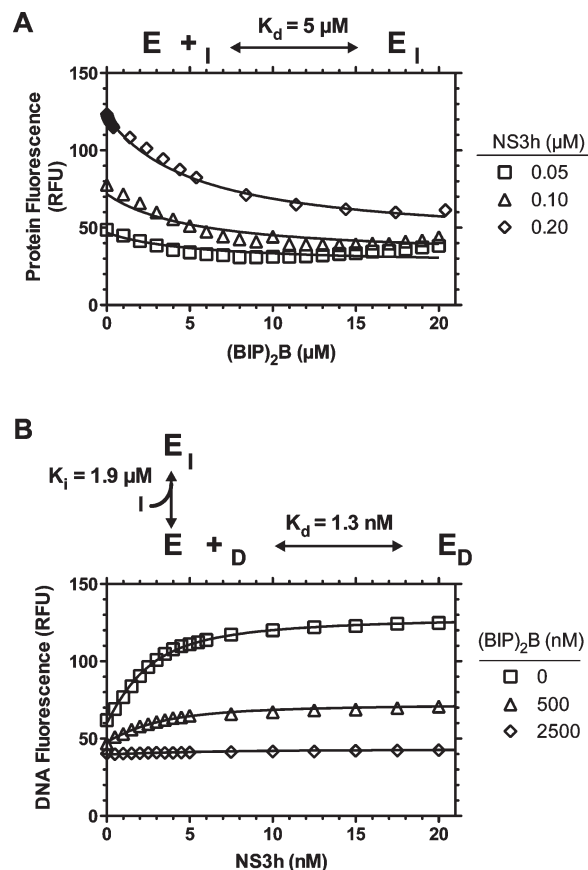


FIGURE 4: Interaction of $(\text{BIP})_2\text{B}$ with enzyme in the absence or presence of DNA. (A) Effect of $(\text{BIP})_2\text{B}$ on NS3h protein fluorescence. The protein fluorescence of a constant concentration of enzyme is measured as a solution is titrated with $(\text{BIP})_2\text{B}$. Corrected fluorescence (F , eq 4) of three different NS3h_1b (con1) solutions was globally fit to eq 5, which assumes a different fluorescence for free enzyme and an enzyme–inhibitor complex described by the coefficients F_f and F_c , respectively. In (B), the fluorescence of 2 nM F18 DNA (5′-GCC TCG CTG CCG TCG CCA-FAM-3′) was measured while titrating with HCV NS3h_1b (con1) in the presence of various concentrations of $(\text{BIP})_2\text{B}$. Data were globally fit to eq 6 to provide an estimate of K_i for the NS3h– $(\text{BIP})_2\text{B}$ complex formation and a K_d for the NS3h–DNA complex.

the constant F_c (eq 5). Since this model only contains enzyme and $(\text{BIP})_2\text{B}$, the possible confounding effects of DNA and ATP are eliminated, and an estimate of the K_d for direct binding of $(\text{BIP})_2\text{B}$ by NS3h can be derived. From this analysis, the K_d for the $(\text{BIP})_2\text{B}$ –NS3h complex was determined to be $5.3 \pm 0.6 \mu\text{M}$ with an F_f of $501 \pm 6 \text{ RFU}/\mu\text{M}$ and an F_c of $92 \pm 18 \text{ RFU}/\mu\text{M}$ and $\text{BGK} = 21.7 \pm 0.9 \text{ RFU}$. Reported errors denote the 95% confidence intervals of the curve fit.

A different technique was used to examine how $(\text{BIP})_2\text{B}$ binding to NS3h might in turn influence NS3h nucleic acid binding. To test the hypothesis that $(\text{BIP})_2\text{B}$ competes with nucleic acid for the same site, we examined how $(\text{BIP})_2\text{B}$ binding to NS3h influences the ability of the enzyme to bind a single-stranded DNA oligonucleotide. NS3h DNA binding can be monitored by measuring the fluorescence of a fluorescein-labeled oligonucleotide in the presence and absence of NS3h (6). The oligonucleotide used here, F18, was an 18 nucleotide long DNA with a 3′ fluorescein label. The fluorescein of F18 is poorly fluorescent at pH less than 7, e.g., in the helicase assay buffer (MOPS, pH 6.5). When bound to NS3h, F18 fluorescence increases, and this change can be used to estimate a dissociation constant (6). To monitor how

(BIP)₂B affects a NS3h–DNA interaction, F18 was titrated with NS3h_1b (con1) in the presence either of 0, 0.5, or 2.5 μ M (BIP)₂B. DNA fluorescence was monitored at these conditions, and data were globally fit to a model that assumes formation of a (BIP)₂B–NS3h complex which does not bind DNA (eq 6). In such a model, the enzyme–DNA complex has a K_d of 1.3 ± 0.2 nM, similar to what has been reported before (6, 21), and the NS3h–(BIP)₂B complex has a K_i of 1.9 ± 1.2 μ M (Figure 4B). Again, reported errors denote the 95% confidence intervals for the curve fit. Such a result is in reasonable agreement with both the IC₅₀'s (0.7–5.4 μ M, Figure 2D) and the K_d for the (BIP)₂B–NS3h complex estimated using intrinsic protein fluorescence (5.3 ± 0.6 μ M, Figure 4A).

Effect of (BIP)₂B on Helicase-Catalyzed ATP Hydrolysis. In the absence of RNA, HCV helicase hydrolyzes ATP (the fuel for unwinding) approximately 100 times slower than HCV helicase hydrolyzes ATP in the presence of saturating amounts of RNA. Poly(U) RNA stimulates ATP hydrolysis most efficiently and to the highest known levels (19). The above data hint that (BIP)₂B binds to HCV helicase in place of DNA (or RNA). If this is the case, then the compound should not affect the ability of the helicase to hydrolyze ATP either in the absence of RNA or in the presence of saturating levels of nucleic acids. It is also possible that (BIP)₂B binds to the helicase and stimulates ATP hydrolysis in the same fashion as RNA.

To examine the effect of (BIP)₂B on NS3h-catalyzed ATP hydrolysis, we measured the liberation of inorganic phosphate from ATP under a variety of conditions. First, to measure effects on ATP hydrolysis in the absence of RNA, reactions were performed for 15 min at 37 °C in 25 mM MOPS, pH 6.5, 1 mM ATP, 5 mM MgCl₂, and 60 nM NS3h_1b (con1). No inhibition was observed with up to 100 μ M (BIP)₂B. When reactions were repeated in the presence of 300 μ M poly(U) RNA under the same conditions as above but with less (1 nM) NS3h_1b (con1), again no inhibition was observed under any condition. A strikingly different effect was observed, however, when ATPase assays are repeated in the presence of RNA at a concentration that produces less than maximal stimulation. For example, at 15 μ M RNA, where the ATPase activity of NS3 is only stimulated to ~30% of its V_{\max} , (BIP)₂B clearly inhibits RNA-stimulated ATPase activity in a dose-dependent manner (data not shown).

When the initial rate of helicase-catalyzed ATP hydrolysis was measured at numerous different concentrations of both RNA and (BIP)₂B, it became clear that the compound and RNA compete with each other (Figure 5A). Basic fits to the Michaelis–Menten equation revealed that (BIP)₂B does not affect the observed V_{\max} , ruling out the possibility that (BIP)₂B interacts with enzyme–RNA–ATP complexes. Rather, the compound affected apparent K_{RNA} , indicative of a competition for the RNA-binding site. Fitting data to a model where (BIP)₂B is assumed to be competitive with RNA (eq 7) revealed a K_i for formation of an unproductive (BIP)₂B–NS3h–ATP complex of 5.0 ± 1.3 μ M, identical within error to the previous K_d estimated for formation of the (BIP)₂B–NS3h complex using intrinsic protein fluorescence (5.3 ± 0.6 μ M, Figure 4A).

We also examined the effect of (BIP)₂B at various ATP concentrations to check if (BIP)₂B competes with the fuel for the unwinding reaction. To evaluate the ability of (BIP)₂B to compete with ATP, we measured rates of helicase-catalyzed ATP hydrolysis in the presence of various concentrations of ATP with fixed concentrations of (BIP)₂B and RNA (15 μ M poly(U))

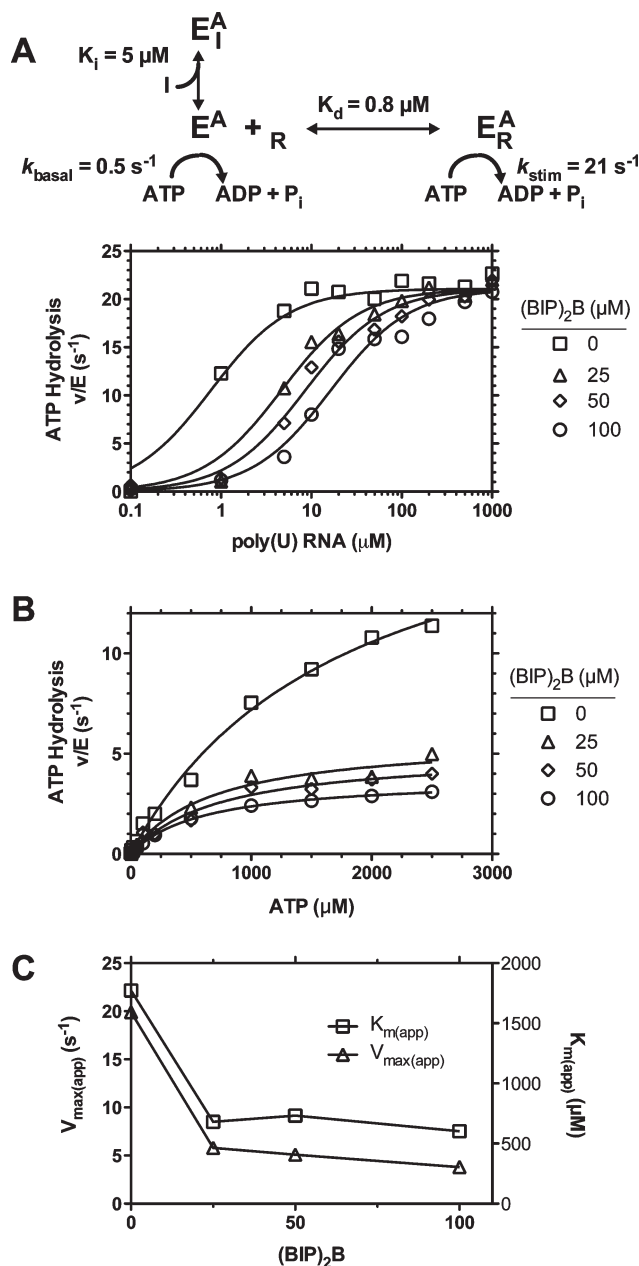


FIGURE 5: Effects of (BIP)₂B on helicase-catalyzed ATP hydrolysis. (A) Stimulation of NS3h_1b (con1) catalyzed ATP hydrolysis by poly(U) RNA in the presence of various concentrations of (BIP)₂B. Note that basal ATPase rate (in the absence of RNA) and maximum ATPase rates are not affected by (BIP)₂B. Only at intermediate concentrations of RNA does (BIP)₂B inhibit ATPase activity. Data are globally fit between data sets using eq 7 to estimate the constants shown. (B) Effect of (BIP)₂B on ATP hydrolysis at various ATP concentrations. Reactions were performed with NS3h_1b (con1) at various ATP concentrations in the presence of 15 μ M poly(U). Data are fit to eq 8. (C) Subplot of apparent K_m 's and V_{\max} 's determined from fits in panel B.

(Figure 5B). Fits to the Michaelis–Menten equation revealed a clear effect on both apparent V_{\max} and K_m (Figure 5C). An effect on apparent V_{\max} indicates that ATP and (BIP)₂B most likely do not compete for the same binding site. The fact that (BIP)₂B also affects the apparent K_m of ATP suggests that the compound does not act like a classical noncompetitive inhibitor but rather as a “mixed” inhibitor that binds both free enzyme and the enzyme–ATP complex, influencing the affinity of the enzyme for ATP. Since nucleic acids are known to modulate the affinity of HCV

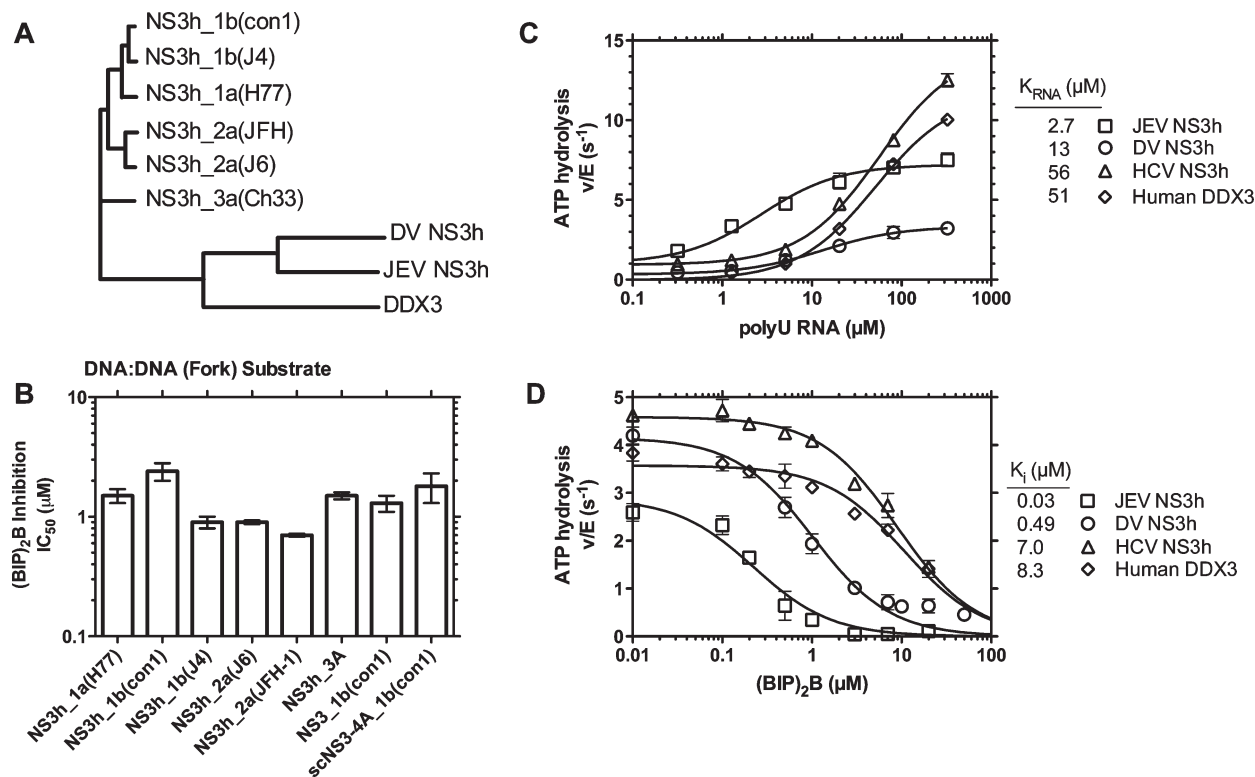


FIGURE 6: Effects of (BIP)₂B on helicases encoded by various HCV genotypes, flaviviruses, and humans. (A) Phylogenetic tree of the hepatitis C virus NS3h proteins used in this study along with NS3h from Dengue virus (DV), NS3h from Japanese encephalitis virus (JEV), and human DDX3 helicase. The tree was drawn from amino acid alignments generated with CLC Sequence Viewer (<http://www.clcbio.com>). (B) Inhibition of HCV helicase-catalyzed DNA–DNA (fork) unwinding by (BIP)₂B, reported as IC₅₀ values with error bars of standard deviation of three independent determinations. “NS3h_x(y)” indicates a truncated NS3 protein lacking a protease domain of HCV genotype x (isolate y). NS3_1b (con1) is the full-length NS3 protein and scNS3–4A_1b (con1) is a full-length NS3 protein with a covalently linked HCV NS4A peptide. (C) RNA-stimulated ATP hydrolysis catalyzed by HCV, JEV, DV, and DDX3 helicases at pH 7.5. The viral HCV, JEV, and DV helicases all exhibit nonzero basal ATPase rates in the absence of RNA while human DDX3 helicase does not detectably hydrolyze ATP in the absence of RNA. Data are fit to eq 9 with each point representing the average of three independent experiments; error bars show standard deviations. (D) Inhibition of ATP hydrolysis by (BIP)₂B when HCV, JEV, DV, and DDX3 helicases are partially stimulated by 15 μM RNA. Data are fit to an equation describing competitive inhibition (eq 10) with each point representing the average of three independent experiments; error bars show standard deviations.

helicase for ATP (21), the observation that (BIP)₂B, which appears to bind in place of nucleic acids, also affects the K_m for ATP is not particularly surprising.

Specificity. Two sets of proteins were used to examine the specificity of (BIP)₂B. The members of the first set were NS3h proteins derived from a variety of HCV genotypes, full-length NS3, and a single chain NS3–NS4A fusion protein (scNS3–4A (10)). The second set was comprised of related helicases encoded by other organisms (Figure 6A). To determine if (BIP)₂B inhibits each of the panels of HCV helicases, standard MBHAs were performed using a variety of DNA and RNA substrates in the presence or absence of 6 μM (BIP)₂B. (BIP)₂B inhibited RNA and DNA unwinding catalyzed by each protein (data not shown). To more rigorously compare the affinity of (BIP)₂B for each HCV protein, assays were repeated with the DNA–DNA(fork) substrate with 11.0, 8.0, 5.5, 3.0, 1.5, 0.7, 0.5, and 0.01 μM (BIP)₂B in triplicate. Percent inhibition at each (BIP)₂B concentration was fit to eq 2 to determine the IC₅₀ values that are shown in Figure 6B. The IC₅₀ values range from 0.7 ± 0.2 μM for the NS3h_2a(JFH-1) protein to 2.4 ± 0.4 μM for the NS3h_1b(con1) protein, a 4-fold difference (Figure 6B). Compared to NS3h_1b(con1), the IC₅₀ seen with NS3h_1a(H77) was slightly lower, at 1.5 ± 0.2 μM, as was the IC₅₀ for reactions performed with NS3h_3a (1.5 ± 0.1 μM). The IC₅₀'s for the NS3h_1b(J4), NS3h_2a(J6), and NS3h_2a(JFH-1) strains were less than half of those noted for the NS3h_1b(con1), at 0.9 ± 0.1 ,

0.9 ± 0.6 , and 0.7 ± 0.2 μM, respectively. Finally, the IC₅₀ values for both the full-length NS3_1b(con1) and scNS3–4A_1b(con1) were slightly lower than that of the reference NS3h_1b(con1) at 1.3 ± 0.2 and 1.8 ± 0.5 μM, respectively (Figure 6B). In all, (BIP)₂B inhibited HCV helicase-catalyzed unwinding similarly, no matter the genotypic origin of the protein, the presence or absence of a protease domain, or the presence or absence of a covalently bound NS4A protease cofactor.

Examining the effect of (BIP)₂B on helicases derived from other species was more difficult because those proteins unwound the MBHA substrates poorly under conditions where HCV helicase was most active (pH 6.5). Since the K_i derived from ATPase assays in competition with RNA closely mimicked the affinity of (BIP)₂B for HCV helicase, we instead used ATPase assays to compare the affinity of (BIP)₂B for each protein. In order to compare the various helicases, we therefore conducted all assays at pH 7.5 in Tris buffer rather than at pH 6.5 in MOPS buffer (the optimal buffer for HCV helicase). At the higher pH, the other proteins were more active, but HCV helicase was less active (30).

To calculate a K_i for (BIP)₂B and each helicase, we first needed to measure the affinity of each protein for activating RNA. RNA affinity was estimated by titrating each protein with RNA and measuring initial rates of ATP hydrolysis (Figure 6C). Rates were converted to specific activities and fit to a one-site binding equation (eq 9) to calculate constants describing the basal rate of helicase-catalyzed ATP hydrolysis (k_{basal}), the maximum

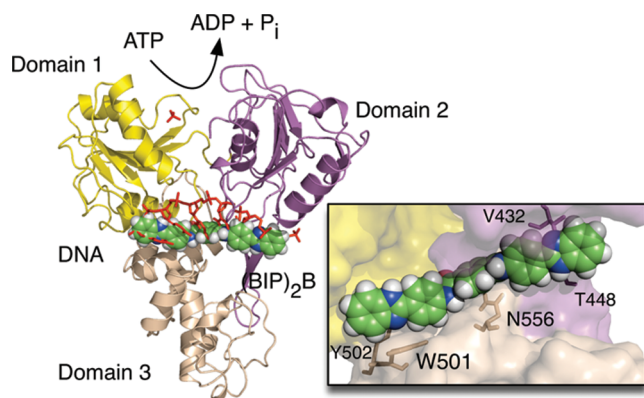


FIGURE 7: Molecular model of $(\text{BIP})_2\text{B}$ bound to the HCV NS3h protein. UCSF DOCK 6.3 was used to bind $(\text{BIP})_2\text{B}$ to the oligonucleotide binding site of PDB structure 1A1V (9). NS3h domains 1, 2, and 3 are represented by yellow, magenta, and tan ribbons, respectively. Bound ligands from PDB 1A1V are shown as red sticks (oligonucleotide and a bound sulfate), and the docked $(\text{BIP})_2\text{B}$ molecule is shown as a space-filling model colored by atom. The insert shows a close-up view of the putative $(\text{BIP})_2\text{B}$ binding site with nearby amino acid side chains labeled.

stimulated rate of ATP hydrolysis (k_{stim}), and the affinity of each helicase for RNA (K_{RNA}). Poly(U) RNA, which is the best activator of HCV NS3h, stimulated ATP hydrolysis catalyzed by all helicases tested. All of the viral proteins also hydrolyzed ATP in the absence of added nucleic acids, i.e., under basal conditions, but the human DDX3 protein had undetectable ATPase activity in the absence of RNA. Notably, both JEV and DV helicases appeared to bind RNA more tightly than either the HCV protein or human DDX3 protein.

Since $(\text{BIP})_2\text{B}$ inhibition of HCV NS3h ATPase activity only occurs at intermediate levels of RNA (i.e., not basal ATPase nor saturated ATPase rates, Figure 5A), we next assessed the ability of $(\text{BIP})_2\text{B}$ to inhibit the ATPase activity of all the other helicases in the presence of limiting (15 μM) poly(U). ATPase assays were carried out in the presence of varying amounts of $(\text{BIP})_2\text{B}$, and data were fit to an equation describing competitive inhibition (eq 10) to calculate a K_i for each helicase (Figure 6D). $(\text{BIP})_2\text{B}$ inhibits the ATPase function of all the helicases, inhibiting both HCV and the human DDX3 proteins with approximately the same potency. However, the compound is a more potent inhibitor of the JEV and DV NS3h enzymes, with the K_i for JEV over 10-fold lower than that seen for HCV under the same conditions.

Docking of $(\text{BIP})_2\text{B}$ and HCV NS3h. On the basis of the above experimental evidence, we next conducted a computational docking simulation to determine what types of interactions $(\text{BIP})_2\text{B}$ could form with the NS3h protein if it indeed bound the nucleic acid binding site in a similar manner as nucleic acid. Ligand docking simulations were done using the program UCSF DOCK 6.3 and molecular surfaces generated from PDB file 1A1V (9) using the program dms. The *a priori* hypothesis was that $(\text{BIP})_2\text{B}$ competes with DNA or RNA; thus the potential ligand binding site was significantly constrained and defined as a region of space within a 3 Å radius of the bound oligonucleotide in the 1A1V structure. Simulations with this stringent constraint suggest that bound $(\text{BIP})_2\text{B}$ occupies almost the entire oligonucleotide binding site with the two benzimidazoles occupying the same nearly vertical plane, and the linking amide–benzene–amide moiety rotated orthogonal to the plane of the benzimidazoles (Figure 7). Apparent ligand–protein interactions include the left-most benzimidazole flanked on either side of the aromatic rings

by W501 (5.0 Å) and Y502 (2.4 Å), the linking benzene sitting over the side chain of N556 (2.9 Å), with V432 (4.4 Å) and T448 (3.4 Å) sitting behind the right-most benzimidazole ring system. No hydrogen bond interactions are immediately apparent, though the front half of the bound ligand is solvent exposed while the back half participates in the hydrophobic interactions noted above.

DISCUSSION

Helicases are complex ATP-fueled molecular motors that track along nucleic acids to displace complementary strands or proteins. Although helicases are needed by all viruses, relatively little progress has been made in exploiting helicases as drug targets. There have been a variety of helicase inhibitors reported in the literature, but few studies have been performed to define the mechanism of action of any of these compounds. Here we investigate the specificity and mechanism of $(\text{BIP})_2\text{B}$, a small molecule inhibitor of the hepatitis C virus NS3 helicase. The potency of $(\text{BIP})_2\text{B}$ in standard helicase assays is roughly comparable to some other recently described small molecule HCV helicase inhibitors such as acridone derivatives (31), amidinoanthracene derivatives (32), triphenylmethane derivatives (33), and the peptide p14 (RRGRTGRGRRGIYR) (34). Our results indicate that $(\text{BIP})_2\text{B}$ directly binds the HCV helicase near the known DNA binding cleft so that the protein no longer forms a functional interaction with its nucleic acid substrate.

Our conclusion that $(\text{BIP})_2\text{B}$ binds in place of RNA (or DNA) is based on four lines of evidence. First, $(\text{BIP})_2\text{B}$ inhibits helicase-catalyzed unwinding *only* when it is premixed with the enzyme–DNA complex (Figure 3A). Second, intrinsic NS3h fluorescence is quenched in the presence of $(\text{BIP})_2\text{B}$ (Figure 4A). Third, DNA fluorescence is no longer enhanced in the presence of NS3h when $(\text{BIP})_2\text{B}$ is present (Figure 4B). Fourth, $(\text{BIP})_2\text{B}$ competes with RNA to inhibit RNA-stimulated ATP hydrolysis (Figure 5A). Although none of these lines of evidence directly locate the $(\text{BIP})_2\text{B}$ binding site, taken together they strongly suggest that $(\text{BIP})_2\text{B}$ binds somewhere in the vicinity of Trp501 in the known NS3h DNA-binding site. Molecular modeling using UCSF DOCK v 6.3 shows that $(\text{BIP})_2\text{B}$ can adopt the proper geometry to bind directly in the known NS3 DNA binding site (9) immediately adjacent to W501 (Figure 7). Such a hypothesis could be further tested using cross-linking, structural studies, or enzyme mutants. Another intriguing possibility is that a single $(\text{BIP})_2\text{B}$ molecule might simultaneously link two NS3 molecules together. To examine this possibility, we have tried to dock $(\text{BIP})_2\text{B}$ with a structure in which two NS3h molecules are bound to the same oligonucleotide (PDB file 2F55 (35)), but the compound is too small to bind two adjacent RNA binding clefts. The linker between the two benzimidazolephenylcarboxamide cores is too short.

Although we can confidently assert that $(\text{BIP})_2\text{B}$ directly binds HCV helicase, it is still not exactly clear how this interaction leads to inhibition of the unwinding reaction. If simple competitive inhibition with the nucleic acid substrate fully explained the mechanism, then the Cheng–Prusoff relationship (36) would predict that an observed IC_{50} must always be greater than the dissociation constant describing the protein–inhibitor interaction. Our best estimate for the affinity of HCV NS3h for $(\text{BIP})_2\text{B}$ comes from monitoring changes in intrinsic protein fluorescence (Figure 4A). However, this dissociation constant (5 μM) exceeds most IC_{50} values determined using unwinding assay. Similarly, plots of percent inhibition in MBHAs versus concentration of $(\text{BIP})_2\text{B}$ fit poorly to a one-site binding equation. Instead, a Hill

coefficient needs to be added to the dose–response equation ($n = 4.5$, Figure 2C) to best fit the data. Again, such a high Hill coefficient might be due to the fact that the HCV helicase unwinds nucleic acids as an oligomer (37) and (BIP)₂B might interact cooperatively with such complexes. However, as mentioned above, the molecular basis for such a cooperative action is still unclear.

Interactions of (BIP)₂B with DNA or RNA might also contribute to its ability to inhibit helicase-catalyzed reactions. For example, the inability of DNA to bind NS3h in the presence of (BIP)₂B (Figure 4B) could be also explained by a model that assumes (BIP)₂B–DNA binding prevents the association of NS3h and DNA. Similarly, (BIP)₂B binding to RNA might explain why more RNA is needed to stimulate helicase-catalyzed ATP hydrolysis in the presence of increasing levels of (BIP)₂B (Figure 5B). It is tempting therefore to try to reconcile all of the data here to a model where (BIP)₂B exerts its action via the substrate rather than the enzyme, but such an explanation is simply not possible for several reasons. First, models for inhibitor–substrate interactions (38) only fit the binding data (Figure 3B) and ATPase data (Figure 4B) if one assumes that (BIP)₂B binds RNA or DNA with a very high affinity (< 1 nM). If (BIP)₂B actually bound RNA or DNA with such a high affinity, one would expect full inhibition when enough (BIP)₂B is added to saturate the substrate, which is present at 5 nM in a MBHA. The observed IC₅₀'s in MBHAs are, however, several orders of magnitude higher (Figure 2). Second, stoichiometric binding to RNA would result in the same IC₅₀ value regardless of which enzyme is present, and this is not observed (Figure 6). Third, if (BIP)₂B bound DNA tightly, it would sequester the trapping oligonucleotide dT₂₀ in single turnover experiments (Figure 3), resulting in multiple turnovers and eventual conversion of all substrate DNA to product. Trap sequestering was never observed, and only approximately 20% of the original 5 nM substrate DNA was utilized (Figure 3). Last, we have also tried to directly measure an interaction between (BIP)₂B and DNA using a fluorescence intercalator displacement assay (39), but no interaction was observed even with 50 μ M (BIP)₂B (data not shown). Thus, although it is possible that (BIP)₂B binds nucleic acids and this interaction contributes to its potency, such an interaction alone cannot explain all the data here.

Cellular experiments indicate (BIP)₂B has little or no inhibitory activity against the HCV replicon (unpublished results). One possible explanation for this observation might be that (BIP)₂B is unable to displace nucleic acid that is already bound to NS3h in cells. Since the K_d for the NS3h–RNA complex is far less than the K_i for the NS3h–(BIP)₂B complex (roughly, 1 nM versus 5 μ M), saturating concentrations of RNA found in replication complexes would easily out-compete (BIP)₂B at the shared binding site, leading to an apparent lack of inhibition when local RNA concentration exceeds the local (BIP)₂B concentration. Similarly, lack of inhibition in cells could be explained by other factors not necessarily related to the structure of the inhibitor *per se*, such as poor absorption of the molecule by cells or rapid cellular metabolism to inactive metabolites. It should be recognized, however, that (BIP)₂B was not the most potent compound in the symmetrical benzimidazolephenyl series of HCV helicase inhibitors. In the 1997 patent, Diana and Bailey identified six compounds with IC₅₀ values over 10 times lower than (BIP)₂B (see Table 1 of U.S. Patent 5,633,388). It might be worthwhile to synthesize and reexamine some related compounds using some of the assays described here.

Finally, we show that, in addition to interacting with HCV helicase, (BIP)₂B inhibits other helicases needed for the replication of other viruses. The fact that (BIP)₂B binds DDX3 with a similar affinity compared to HCV helicase suggests that (BIP)₂B or similar compounds might be found that exert some anti-HIV effect. Most notable, however, is the discovery that (BIP)₂B binds the flavivirus NS3h proteins considerably more tightly than HCV NS3h, suggesting that compounds in the symmetrical benzimidazolephenyl series might actually be more valuable as potential anti-flaviviral agents. Some of the assays and methods described here could be used to screen (BIP)₂B derivatives or similar compounds for such antiviral agents.

ACKNOWLEDGMENT

We thank Fred Jaffe for valuable technical assistance and Brett Lindenbach, Julien Lescar, Bruno Coutard, Violaine Lantéz and Bruno Canard for generously providing plasmids. The expression plasmid for the JEV helicase was produced as part of the European Virus Archive (EVA) project (European FP7 Capacities Project no 228292, <http://www.european-virus-archive.com/>).

REFERENCES

1. Kwong, A. D., Rao, B. G., and Jeang, K. T. (2005) Viral and cellular RNA helicases as antiviral targets. *Nat. Rev. Drug Discov.* 4, 845–853.
2. Frick, D. N., and Lam, A. M. (2006) Understanding helicases as a means of virus control. *Curr. Pharm. Des.* 12, 1315–1338.
3. Frick, D. N. (2007) The hepatitis C virus NS3 protein: a model RNA helicase and potential drug target. *Curr. Issues Mol. Biol.* 9, 1–20.
4. Belon, C. A., and Frick, D. N. (2009) Helicase inhibitors as specifically targeted antiviral therapy for hepatitis C. *Future Virol.* 4, 277–293.
5. Phoon, C. W., Ng, P. Y., Ting, A. E., Yeo, S. L., and Sim, M. M. (2001) Biological evaluation of hepatitis C virus helicase inhibitors. *Bioorg. Med. Chem. Lett.* 11, 1647–1650.
6. Frick, D. N., Rypma, R. S., Lam, A. M., and Gu, B. (2004) The nonstructural protein 3 protease/helicase requires an intact protease domain to unwind duplex RNA efficiently. *J. Biol. Chem.* 279, 1269–1280.
7. Beran, R. K., Serebrov, V., and Pyle, A. M. (2007) The serine protease domain of hepatitis C viral NS3 activates RNA helicase activity by promoting the binding of RNA substrate. *J. Biol. Chem.* 282, 34913–34920.
8. Beran, R. K., Lindenbach, B. D., and Pyle, A. M. (2009) The NS4A protein of hepatitis C virus promotes RNA-coupled ATP hydrolysis by the NS3 helicase. *J. Virol.* 83, 3268–3275.
9. Kim, J. L., Morgenstern, K. A., Griffith, J. P., Dwyer, M. D., Thomson, J. A., Murcko, M. A., Lin, C., and Caron, P. R. (1998) Hepatitis C virus NS3 RNA helicase domain with a bound oligonucleotide: the crystal structure provides insights into the mode of unwinding. *Structure* 6, 89–100.
10. Yao, N., Reichert, P., Taremi, S. S., Prosise, W. W., and Weber, P. C. (1999) Molecular views of viral polyprotein processing revealed by the crystal structure of the hepatitis C virus bifunctional protease-helicase. *Struct. Folding Des.* 7, 1353–1363.
11. Simmonds, P. (2004) Genetic diversity and evolution of hepatitis C virus—15 years on. *J. Gen. Virol.* 85, 3173–3188.
12. Fried, M. W., Shiffman, M. L., Reddy, K. R., Smith, C., Marinos, G., Goncales, F. L. J., Haussinger, D., Diago, M., Carosi, G., Dhumeaux, D., Craxi, A., Lin, A., Hoffman, J., and Yu, J. (2002) Peginterferon alfa-2a plus ribavirin for chronic hepatitis C virus infection. *N. Engl. J. Med.* 347, 975–982.
13. Thibault, D., Bousquet, C., Gingras, R., Lagace, L., Maurice, R., White, P. W., and Lamarre, D. (2004) Sensitivity of NS3 serine proteases from hepatitis C virus genotypes 2 and 3 to the inhibitor BILN 2061. *J. Virol.* 78, 7352–7359.
14. Pauwels, F., Mostmans, W., Quirynen, L. M., van der Helm, L., Boutton, C. W., Rueff, A. S., Cleiren, E., Raboisson, P., Surleraux, D., Nyanguile, O., and Simmen, K. A. (2007) Binding site identification and genotypic profiling of hepatitis C virus polymerase inhibitors. *J. Virol.* 81, 6909–6919.

15. Luo, D., Xu, T., Watson, R. P., Scherer-Becker, D., Sampath, A., Jahnke, W., Yeong, S. S., Wang, C. H., Lim, S. P., Strongin, A., Vasudevan, S. G., and Lescar, J. (2008) Insights into RNA unwinding and ATP hydrolysis by the flavivirus NS3 protein. *EMBO J.* 27, 3209–3219.
16. Luo, D., Xu, T., Hunke, C., Gruber, G., Vasudevan, S. G., and Lescar, J. (2008) Crystal structure of the NS3 protease-helicase from dengue virus. *J. Virol.* 82, 173–183.
17. Yedavalli, V. S., Neuveut, C., Chi, Y. H., Kleiman, L., and Jeang, K. T. (2004) Requirement of DDX3 DEAD box RNA helicase for HIV-1 Rev-RRE export function. *Cell* 119, 381–392.
18. Yedavalli, V. S., Zhang, N., Cai, H., Zhang, P., Starost, M. F., Hosmane, R. S., and Jeang, K. T. (2008) Ring expanded nucleoside analogues inhibit RNA helicase and intracellular human immunodeficiency virus type 1 replication. *J. Med. Chem.* 51, 5043–5051.
19. Lam, A. M., Keeney, D., Eckert, P. Q., and Frick, D. N. (2003) Hepatitis C virus NS3 ATPases/helicases from different genotypes exhibit variations in enzymatic properties. *J. Virol.* 77, 3950–3961.
20. Neumann-Haefelin, C., Frick, D. N., Wang, J. J., Pybus, O. G., Salloum, S., Narula, G. S., Eckart, A., Biezynski, A., Eiermann, T., Klennerman, P., Viazov, S., Roggendorf, M., Timme, R., Reiser, M., and Timm, J. (2008) Analysis of the evolutionary forces in an immunodominant CD8 epitope in hepatitis C virus at a population level. *J. Virol.* 82, 3438–3451.
21. Frick, D. N., Banik, S., and Rypma, R. S. (2007) Role of divalent metal cations in ATP hydrolysis catalyzed by the hepatitis C virus NS3 helicase: magnesium provides a bridge for ATP to fuel unwinding. *J. Mol. Biol.* 365, 1017–1032.
22. Belon, C. A., and Frick, D. N. (2009) Fuel specificity of the hepatitis C virus NS3 helicase. *J. Mol. Biol.* 388, 851–864.
23. Lindenbach, B. D., Evans, M. J., Syder, A. J., Wolk, B., Tellinghuisen, T. L., Liu, C. C., Maruyama, T., Hynes, R. O., Burton, D. R., McKeating, J. A., and Rice, C. M. (2005) Complete replication of hepatitis C virus in cell culture. *Science* 309, 623–626.
24. Xu, T., Sampath, A., Chao, A., Wen, D., Nanao, M., Chene, P., Vasudevan, S. G., and Lescar, J. (2005) Structure of the dengue virus helicase/nucleoside triphosphatase catalytic domain at a resolution of 2.4 Å. *J. Virol.* 79, 10278–10288.
25. Speroni, S., De Colibus, L., Mastrangelo, E., Gould, E., Coutard, B., Forrester, N. L., Blanc, S., Canard, B., and Mattevi, A. (2008) Structure and biochemical analysis of Kokobera virus helicase. *Proteins* 70, 1120–1123.
26. Lanzetta, P. A., Alvarez, L. J., Reinach, P. S., and Candia, O. A. (1979) An improved assay for nanomole amounts of inorganic phosphate. *Anal. Biochem.* 100, 95–97.
27. Belon, C. A., and Frick, D. N. (2008) Monitoring helicase activity with molecular beacons. *BioTechniques* 45, 433–440/442.
28. Preugschat, F., Averett, D. R., Clarke, B. E., and Porter, D. J. (1996) A steady-state and pre-steady-state kinetic analysis of the NTPase activity associated with the hepatitis C virus NS3 helicase domain. *J. Biol. Chem.* 271, 24449–24457.
29. Lam, A. M., Keeney, D., and Frick, D. N. (2003) Two novel conserved motifs in the hepatitis C virus NS3 protein critical for helicase action. *J. Biol. Chem.* 278, 44514–44524.
30. Lam, A. M., Rypma, R. S., and Frick, D. N. (2004) Enhanced nucleic acid binding to ATP-bound hepatitis C virus NS3 helicase at low pH activates RNA unwinding. *Nucleic Acids Res.* 32, 4060–4070.
31. Manfroni, G., Paeshuyse, J., Massari, S., Zanolli, S., Gatto, B., Maga, G., Tabarrini, O., Cecchetti, V., Fravolini, A., and Neyts, J. (2009) Inhibition of subgenomic hepatitis C virus RNA replication by acridone derivatives: identification of an NS3 helicase inhibitor. *J. Med. Chem.* 52, 3354–3365.
32. Krawczyk, M., Wasowska-Lukawska, M., Oszczapowicz, I., and Boguszewska-Chachulska, A. M. (2009) Amidinoanthracyclines—a new group of potential anti-hepatitis C virus compounds. *Biol. Chem.* 390, 351–360.
33. Chen, C. S., Chiou, C. T., Chen, G. S., Chen, S. C., Hu, C. Y., Chi, W. K., Chu, Y. D., Hwang, L. H., Chen, P. J., Chen, D. S., Liaw, S. H., and Chern, J. W. (2009) Structure-based discovery of triphenylmethane derivatives as inhibitors of hepatitis C virus helicase. *J. Med. Chem.* 52, 2716–2723.
34. Gozdek, A., Zhukov, I., Polkowska, A., Poznanski, J., Stankiewicz-Drogon, A., Pawlowicz, J. M., Zagorski-Ostojka, W., Borowski, P., and Boguszewska-Chachulska, A. M. (2008) NS3 peptide, a novel potent hepatitis C virus NS3 helicase inhibitor: its mechanism of action and antiviral activity in the replicon system. *Antimicrob. Agents Chemother.* 52, 393–401.
35. Mackintosh, S. G., Lu, J. Z., Jordan, J. B., Harrison, M. K., Sikora, B., Sharma, S. D., Cameron, C. E., Raney, K. D., and Sakon, J. (2006) Structural and biological identification of residues on the surface of NS3 helicase required for optimal replication of the hepatitis C virus. *J. Biol. Chem.* 281, 3528–3535.
36. Cheng, Y., and Prusoff, W. H. (1973) Relationship between the inhibition constant (K_i) and the concentration of inhibitor which causes 50% inhibition (I₅₀) of an enzymatic reaction. *Biochem. Pharmacol.* 22, 3099–3108.
37. Jennings, T. A., Mackintosh, S. G., Harrison, M. K., Sikora, D., Sikora, B., Dave, B., Tackett, A. J., Cameron, C. E., and Raney, K. D. (2009) NS3 helicase from the hepatitis C virus can function as a monomer or oligomer depending on enzyme and substrate concentrations. *J. Biol. Chem.* 284, 4806–4814.
38. Copeland, R. A., and Horiuchi, K. Y. (1998) Kinetic effects due to nonspecific substrate-inhibitor interactions in enzymatic reactions. *Biochem. Pharmacol.* 55, 1785–1790.
39. Boger, D. L., Fink, B. E., Brunette, S. R., Tse, W. C., and Hedrick, M. P. (2001) A simple, high-resolution method for establishing DNA binding affinity and sequence selectivity. *J. Am. Chem. Soc.* 123, 5878–5891.